



# Neural correlates of metacontrast masking across different contrast polarities

Alaz Aydin<sup>1,2</sup> · Haluk Ogmen<sup>3</sup> · Hulusi Kafaligonul<sup>1,4</sup>

Received: 7 September 2020 / Accepted: 16 March 2021 / Published online: 29 March 2021  
© The Author(s), under exclusive licence to Springer-Verlag GmbH Germany, part of Springer Nature 2021

## Abstract

Metacontrast masking is a powerful illusion to investigate the dynamics of perceptual processing and to control conscious visual perception. However, the neural mechanisms underlying this fundamental investigative tool are still debated. In the present study, we examined metacontrast masking across different contrast polarities by employing a contour discrimination task combined with EEG (Electroencephalography). When the target and mask had the same contrast polarity, a typical U-shaped metacontrast function was observed. A change in mask polarity (i.e., opposite mask polarity) shifted this masking function to a monotonic increasing function such that the target visibility was strongly suppressed at stimulus onset asynchronies less than 50 ms. This transition in metacontrast function has been typically interpreted as an increase in intrachannel inhibition of the sustained activities functionally linked to object visibility and identity. Our EEG analyses revealed an early (160–300 ms) and a late (300–550 ms) spatiotemporal cluster associated with this effect of polarity. The early cluster was mainly over occipital and parieto-occipital scalp sites. On the other hand, the later modulations of the evoked activities were centered over parietal and centro-parietal sites. Since both of these clusters were beyond 160 ms, the EEG results point to late recurrent inhibitory mechanisms. Although the findings here do not directly preclude other proposed mechanisms for metacontrast, they highlight the involvement of recurrent intrachannel inhibition in metacontrast masking.

**Keywords** Visual masking · Metacontrast · Contour discrimination · Contrast polarity · ON–OFF pathways · EEG

## Introduction

Visual masking as a phenomenon has been known for more than a century and also has found increasing applications as a powerful methodological tool in studies of information processing and conscious perception (Bachmann and Francis 2013; Breitmeyer and Ogmen 2006). A particular case

of masking, which probably attracted the attention of most researchers in the field, is called metacontrast. Metacontrast masking is a type of backward masking in which the visibility of a visual target is suppressed by a spatially contiguous stimulus called the mask. Target visibility is plotted against various stimulus onset asynchronies (SOAs). The strength of masking (i.e., the decrease of target visibility) is typically a U-shaped function of SOA (Bachmann 1994; Breitmeyer and Ogmen 2000, 2006). The specific morphology of this function (e.g., the location of dips, the amount of reduction in target visibility) depends on stimulus variables, the criterion content, and the perceptual task. Therefore, changes in masking functions have been used to probe the dynamics of vision, including processing streams, specialized for different visual attributes and the interactions between these streams at different stages (Breitmeyer et al. 2004, 2006; Ogmen et al. 2003).

Employing this common approach, previous studies (Breitmeyer 1978a; Breitmeyer et al. 2008; Sherrick et al. 1974) reported that substantial U-shaped masking functions can be obtained even when the target and mask have opposite

---

✉ Hulusi Kafaligonul  
hulusi@bilkent.edu.tr

<sup>1</sup> National Magnetic Resonance Research Center (UMRAM), Bilkent University, Ankara, Turkey

<sup>2</sup> Department of Cognitive Science, Informatics Institute, Middle East Technical University, Ankara, Turkey

<sup>3</sup> Laboratory of Perceptual and Cognitive Dynamics, Electrical and Computer Engineering, Ritchie School of Engineering and Computer Science, University of Denver, Denver, CO, USA

<sup>4</sup> Interdisciplinary Neuroscience Program, Aysel Sabuncu Brain Research Center, Bilkent University, 06800 Ankara, Turkey

contrast polarities. Moreover, the masking strength in these conditions was overall weaker compared to the same polarity conditions, indicating that metacontrast is also contrast polarity specific, but such specificity is partial and not absolute. These behavioral findings provide interesting and novel implications for visual processing. First, metacontrast masking across different polarities points to a significant interaction (i.e., inhibition) between ON and OFF pathways specialized for processing brightness increments and decrements, respectively (Schiller 1992). Second, they also suggest that this interaction across pathways may have distinct characteristics than the one elicited by metacontrast within each (ON or OFF) channel. How cross-polarity metacontrast is mediated in the visual system remains unanswered. In masking studies, the dual-channel, sustained-transient approach has been shown to have a broad explanatory scope (Breitmeyer and Ogmen 2000). This approach addresses timing differences between transient and sustained activities of M (magnocellular/magno-dominant) and P (parvocellular/parvo-dominant) channels, respectively. According to models based on this theory, the transient and sustained activities of the mask suppress the sustained (visibility) activity of the target via the feedforward interaction between these channels and the inhibitions (e.g., lateral and recurrent) within the P channel. Although both inter- and intra-channel inhibitory mechanisms contribute to metacontrast masking, the dominant one is inter-channel inhibition. Within the framework of the dual-channel approach, the cross-polarity metacontrast can be illustrated by incorporating ON and OFF pathway interactions. Schiller (1982) demonstrated the existence of separate ON and OFF populations within both P and M channels. A possible mechanism may be inhibitory coupling from transient (M) onto sustained (P) neurons. In other words, on-transient (and, similarly, off-transient) neurons can form inhibitory connections with both on- and off-sustained neurons. Early neurophysiological recordings also revealed that complex-cell types in the monkey primary visual cortex (V1) are sensitive to both luminance increments and decrements (Hubel and Wiesel 1968; Schiller et al. 1976). More importantly, a subset of these increment- and decrement-sensitive complex cells have short-latency phasic (i.e., transient) activities (Dow 1974). Such neurons may provide a basis not only for inter-channel inhibition but also for across polarity interaction to obtain significant metacontrast. Alternatively, it is also possible that the interaction between two polarities may be mainly within the P pathway (e.g., an inhibition between on-sustained and off-sustained populations) and hence lead to metacontrast masking with distinct characteristics. However, these alternatives and specific neural correlates have not been investigated yet.

Given that visual masking is a dynamic process, often studied by stimuli of short duration, the neural correlates of metacontrast have been commonly investigated through

neuroimaging techniques with a high temporal resolution like Electroencephalography (EEG). Initial studies focused on whether metacontrast leads to significant alterations in the early (< 100 ms) components (e.g., C1 and C2) which are associated with the early processing over V1 and receive major contributions from the earliest retinotopic regions of visual processing (Donchin et al. 1963; Jeffreys and Mussetwhite 1986; Schiller and Chorover 1966). Although no substantial effects of metacontrast on these components were reported, relatively recent research pointed to significant changes in relatively late components. Some of these EEG studies emphasized that the changes around 100 ms after the target onset (P1 component, a relatively late response component of V1 cortical response) are important for metacontrast and more generally backward masking (Fahrenfort et al. 2007; Rieger et al. 2005; Sterkin et al. 2009). There are also studies highlighting the importance of later components. Notably, most of the studies provide evidence that the modulations between 200 and 300 ms play a critical role in metacontrast masking [Bridgeman 1988; Koivisto and Grassini 2016; Railo and Koivisto 2009; see also an MEG (Magneto-encephalography) study by Van Aalderen-Smeets et al. (2006)]. Previous studies also indicate significant alterations beyond 300 ms such as late positivity (LP). Since these identified time-ranges have been considered as not reflecting early sensory processing, EEG research on metacontrast highlights late inhibitory mechanisms (e.g., recurrent inhibitions) rather than early feedforward inhibitions. It should also be noted that the variations across these studies were high in terms of criterion content and perceptual task used. The effects of metacontrast on the neural activities still need to be examined by using low-level stimulus manipulations, which are critical for the specific morphology of masking function. Based on previous metacontrast findings (e.g., Breitmeyer et al. 2008), the contrast polarity can be used as a low-level stimulus manipulation to address this gap in neurophysiological studies (see below).

In the present study, we focused on understanding the neural correlates of metacontrast masking across different polarities. We acquired EEG activity while participants performed a contour discrimination task on a visual target under different polarity and SOA conditions. Comparing the cross-polarity masking effects with those of the same polarity conditions, we wanted to determine common and distinct characteristics of cross-polarity metacontrast in the spatiotemporal (i.e., scalp-site and time-domain) profile of the neural activity. Although previous behavioral studies have extensively investigated visual masking under a rich profile of visual stimulations and criterion contents, there are still limited neurophysiological recordings. In terms of neural mechanisms underlying metacontrast, this has led to a mismatch between the recording studies and the theoretical work mainly based on behavioral findings. As mentioned

above, a change in mask polarity is an influential low-level stimulus manipulation on the final masking function. Using mask polarity as a critical experimental factor, we also wanted to identify modulations of ERP components that parallel changes in the masking functions. Thus, we aimed to bridge this gap between neurophysiological and theoretical studies on metacontrast.

## Materials and methods

### Behavioral pre-study

The masking functions are highly dependent on stimulus parameters and criterion content used. Using the basic parameters of the main EEG experiment, we designed a behavioral pre-study to evaluate masking functions of the same and opposite polarity conditions within a wide range of SOA values. Thus, we aimed to identify critical SOA conditions for the EEG experiment. Twenty-four healthy volunteers participated in this study. The data of five participants were excluded from analysis because their performances did not meet our criterion in the contour discrimination task (see “[Design and procedure](#)”). Thus, the data from 19 observers (age range 20–32 years) were included in the analysis. All observers had normal or corrected-to-normal visual acuity, and none of them had a history of neurological disorders. Prior to their participation, they were informed about the experimental procedures and gave informed consent. All experimental procedures were in accordance with the Declaration of Helsinki (World Medical Association 2013) and approved by the local ethics committee at Bilkent University.

### Apparatus and stimuli

We used MATLAB version 8.5 (The MathWorks, Natick, MA, USA) with Psychtoolbox 3.0 (Brainard 1997; Kleiner et al. 2007; Pelli 1997) to control visual stimulation, experimental design, and data acquisition. The stimuli were presented on a 20-inch CRT screen (1280 × 1024 pixel resolution and 100 Hz refresh rate) at a viewing distance of approximately 57 cm. The display was gamma-corrected using a SpectroCAL (Cambridge Research Systems, Rochester, Kent, UK) photometer. A digital oscilloscope (Rigol DS 10204B, GmbH, Puchheim, Germany) with a photodiode was used to check and calibrate the timing of visual stimuli. All the experiments were performed in a silent and dimly lit room.

A red fixation target was presented at the center of the screen. To minimize eye movements during fixation, it was the combination of a bull’s eye and crosshair (Thaler et al. 2013), with 0.6° and 0.2° diameters of outer and inner circles, respectively. The target and mask were centered 3°

above the fixation on the vertical meridian (Fig. 1). The target was a disk of 1.5° diameter with a 0.15° wide right or left contour deletion. The mask ring had 1.55° inner and 2.55° outer diameters, and it surrounded the target disk. These parameters led to a target-mask separation of 0.05°. This target-mask separation was carefully adjusted to prevent any merging of task and mask and a possible pop-out of contour deletion at short SOAs. Upon debriefing, all the participants confirmed that they perceived target and mask as separate in all SOAs. The background was a uniform gray field with a fixed luminance of 45 cd/m<sup>2</sup>. The target was displayed at a luminance of 80 cd/m<sup>2</sup> yielding a white stimulation. However, the mask had a luminance of either 80 cd/m<sup>2</sup> (white) or 10 cd/m<sup>2</sup> (black) to have the same and opposite polarity conditions, respectively. These luminance values resulted in equal Weber contrasts for both polarity conditions (Breitmeyer et al. 2008). The target and mask stimuli had the same duration of 20 ms.

### Design and procedure

We employed a (2 × 9) repeated-measures design, in which we varied the mask polarity (white vs. black; equivalently same vs. opposite polarity) and SOA (0, 10, 20, 40, 60, 80, 120, 160, 200 ms) between target and mask. Our design also included a target-only (baseline) condition where the target was presented without a mask (Fig. 1). Each experimental session had a balanced mixture of these conditions and consisted of 380 trials (19 conditions × 20 trials per condition). Of the 20 trials per condition, 10 were devoted to each of the two possible target contours (left vs. right contour deletion). The order of target contours was randomized across the 20 trials.

On each trial, a condition was pseudo-randomly selected and presented according to the timelines in Fig. 1. A trial started with the presentation of fixation, and after a variable pre-stimulus interval (1000 ± Δ ms, with 0 ≤ Δ ≤ 150), the target and mask sequence (TM+ or TM-) was shown. A maximum response time of 1000 ms following the mask offset was given to observers, and then the fixation disappeared. For the target-only condition, the maximum response time was based on the target offset. Observers were asked to fixate during a trial and to indicate, by pressing one of two keys, which of the two targets was presented before the fixation disappears (i.e., contour discrimination task). In case of no response within the given period, the trial was repeated later in the session. As in the pre-stimulus interval, a variable inter-trial interval (1000 ± Δ ms, with 0 ≤ Δ ≤ 150). The contour discrimination task was employed based on the previous findings indicating that this perceptual task reflects changes in target visibility due to both paracontrast and metacontrast (Breitmeyer 1978a; Breitmeyer et al. 2006; Kafaligönül et al. 2009). In particular, Breitmeyer et al. (2006) used both



**Fig. 1** Schematic representation of stimuli and timeline. Each condition is represented in separate rows. The target was a disk with either left or right contour deletion. The mask annulus surrounded the target disk, and it was presented at different stimulus onset asynchronies.

Both stimuli were displayed  $3^\circ$  above the red fixation. All conditions were used in the EEG study. Only the target-mask (TM+, TM-) and target-only (T) conditions were included in the behavioral pre-study (rows 2, 5, 6)

brightness matching (i.e., direct assessment of target visibility) and contour discrimination tasks in the same experimental design. They directly compared the masking functions across these tasks under different M/T contrast ratios (i.e., direct manipulation of stimulation visibility). In terms of the overall morphology of metacontrast masking functions, the contour discrimination task was in line with the brightness matching task and revealed/captured changes in target visibility well.

Each observer completed a single experimental session. Prior to this experimental session, all possible target-mask configurations were shown to instruct the task and to provide examples of visual stimulation. The participants were also informed about the limited time window to respond, and the importance of fixation was emphasized. They were also screened according to the performance in the target-only condition, and a participant having performance below 75% threshold level was excluded from further data analysis.

## Behavioral data analysis

We first calculated the average performance values of all conditions. For each observer, the average performance value of the target-only was subtracted from those at each SOA and mask polarity condition. This subtraction procedure allowed us to eliminate potential confounding factors and to observe the main masking effect in the contour discrimination task. We performed a two-way repeated-measures ANOVA with polarity and SOA as factors on these difference ( $\Delta$ ) performance values.

## EEG study

### Design and procedure

Based on the performance values in the pre-study, we identified three critical SOA values (10, 50, and 200 ms; see also “Results”), Fig. 2. Accordingly, we only used these SOA values (2 polarity  $\times$  3 SOA conditions) for the main EEG experiment. In our ERP analyses, we used an additive model to detect nonlinear neural response interactions and to reveal modulations of these nonlinear components by experimental factors (see ERP analyses). Therefore, the design also included mask-only (M+ or M−) and no-stimulus (NS) conditions. The timeline and event markers in these conditions were the same as those in the target-only (T) condition, but the stimulation was different (Fig. 1). To avoid potential confounding factors in our analyses, the observers were instructed not to respond and passively fixate when there was no target during a trial (i.e., M or NS trials). Each condition was repeated 60 times per session. Accordingly, there were 600 trials (10 conditions  $\times$  60 trials per condition) in each experimental session. During an experimental session, the target (i.e., T, TM+, TM−) and non-target trials (i.e., M+, M−, NS) were presented in two separate blocks of trials. The order of these blocks and the conditions in each block were randomized. Each observer completed one experimental session. With the exception of these changes, all other stimulus parameters and experimental procedures were the same as those used in behavioral pre-study. We invited all 19 observers of behavioral pre-study to the main EEG experiment, and 14 of them returned and took part in EEG recordings. We did not apply for any additional screening.

### EEG recording and preprocessing

We used the same testing room and behavioral set-up for the EEG study. EEG recording and preprocessing steps were also similar to those described previously (Akyuz et al. 2020; Kaya and Kafaligonul 2019). EEG activity was recorded via a 64-channel system (Brain Products, GmbH, Gilching, Germany). In this system, the scalp electrodes (Ag/AgCl passive

electrodes) were mounted on an elastic cap (BrainCap MR, Brain Products, GmbH), and their arrangement was according to the extended 10/20 system. An additional electrode was placed on the back of the subjects for electrocardiogram (ECG) recording. Two of the scalp electrodes were used as the reference (FCz) and ground (AFz). Electrode impedances were kept below 10 k $\Omega$  by applying a conductive paste (ABRALYT 2000, FMS, Herrsching–Breitbrunn, Germany) with syringe and q-tips. EEG signals were acquired at a 1-kHz sampling rate, and band-pass-filtered between 0.016 and 250 Hz. BrainVision Recorder Software (Brain Products, GmbH) was used to store neural signals, stimulus markers, and observer responses.

Preprocessing of EEG data was carried out offline with the Brainstorm toolbox (Tadel et al. 2011). First, the large and unused segments (e.g., session breaks) were removed, and the data was down-sampled to 500 Hz. The power spectrum was also monitored to identify any significantly noisy channel. Afterward, the data were offline re-referenced to a common average, and a second order IIR notch filter with zero-phase lag was applied for power-line contaminations at 50 Hz. A linear phase FIR band-pass filter was also applied at 0.5 and 70 Hz cut-off frequencies. Eye blinks and heartbeats were detected using frontal channels and the ECG recordings, respectively. To remove common artifacts (e.g., eye blinks and residual heartbeat components), the signal-space projection (SSP) method was used (Uusitalo and Ilmoniemi 1997). Components were screened for the correlation with typical characteristics of common artifacts in their spatial topography and time series. In the end, the data were divided into epochs regarding trials and stimulus onset events centered at zero within a (− 600, 1200) ms window. Trials were screened manually for undetected artifacts, and those which included blinks concurrent with stimulus presentations were also rejected. On average, 95.05% of the trials (SD = 0.04%) were preserved.

### ERP analyses

To compute event-related potential (ERP) for each condition of a participant, the preprocessed signals from each electrode location were averaged across trials and then baseline-corrected by using the mean of 100 ms pre-stimulus period. To further smooth the ERPs, a low pass filter (a linear phase FIR filter with 40 Hz cut-off frequency) was applied. In metacontrast masking, the participants perform a visual task on the target and passively observe the mask. That is to say, the target and mask act as primary task-relevant and secondary task-irrelevant stimulation, respectively. Such experimental design implies that the mask (i.e., secondary stimulation) interferes and interacts with the sensory processing primarily driven by the target. Moreover, most

of the masking theories emphasize nonlinear interactions between the representations of the target and the mask by taking into account the temporal properties of these visual stimuli (Francis 2000). Therefore, as in previous studies (e.g., Del Cul et al. 2007; Fahrenfort et al. 2007), we used derived waveforms for further analyses. We mainly aimed at isolating nonlinear neural interactions and revealing the modulations of these nonlinear components by polarity and SOA. In this respect, we compared the ERPs elicited by target-mask sequence (TM+, TM−) with the synthetic summation of target-only (T) and corresponding mask-only (M+, M−) ERPs. Since the observers passively fixated during mask-only trials, we avoided specific confounding factors due to summation (e.g., having two motor responses in the summed ERPs). Similar to previous research using onset timing as a critical experimental factor (e.g., Cecere et al. 2017), we shifted the mask-only waveforms in time to match the three distinct SOAs used for the corresponding TM conditions. We also applied an additional correction to limit the contribution of confounding factors in the summed ERPs, which could be mistaken for genuine interaction when these ERPs were compared with those of corresponding TM trials. Any pre-stimulus anticipatory slow potential (e.g., contingent negative variation, Walter et al. 1964) might continue after the stimulus onset on all trials. Similarly, the summed ERPs would contain two slow potentials, and it would be inappropriate to compare these ERPs with those of TM trials. To balance such pre-stimulus common activity, we also subtracted the activities of NS trials from synthetic summation [TM vs. (T + M − NS)].

These synthetic ERPs were subtracted from the corresponding TM conditions to quantify nonlinear interactions. Accordingly, the difference [TM − (T + M − NS)] waveforms for each polarity and SOA condition were computed. For each SOA condition, we performed running paired samples *t* tests (same vs. opposite polarity) on these difference waveforms to determine the spatiotemporal profile of significant modulations by contrast polarity. To overcome multiple comparisons across time points and electrode locations at the cluster-level, we used the cluster-based permutation test integrated into Brainstorm and Fieldtrip toolboxes (Maris and Oostenveld 2007). Briefly, we selected a priori time-ranges as 50–300 ms and 300–550 ms for early and late activities reported by previous studies (Bridgeman 1988; Fahrenfort et al. 2007; Railo and Koivisto 2009). Within each time-range, spatially- and temporally-adjacent significant ( $\alpha = 0.05$ ) samples (electrode location, time point) were clustered. The cluster-level statistics were obtained by summing *t* values within a spatiotemporal cluster. To generate the null distribution of the cluster-level statistics, the procedure was repeated using Monte Carlo simulations with 10,000 random permutations of the original data. In the end, the observed (i.e., empirical) cluster-level statistics were

compared to the generated null-distribution. The observed statistics were considered to be significant when it fell in the highest or the lowest 2.5th percentile of the generated null-distribution.

Based on the outcome of the cluster-based permutation test, we identified spatiotemporal clusters associated with the significant effects of contrast polarity for each SOA condition. We further determined electrode locations (i.e., exemplar sites) to display evoked brain activity time-courses for illustrative purposes. The electrodes, which were part of a significant spatiotemporal cluster when it was at its largest spatial extent (in terms of the number of electrodes), were selected as exemplar sites. For the time windows in which the identified spatiotemporal clusters were mainly located, we computed the mean difference [TM − (T + M − NS)] waveforms over these electrodes. We carried out correlation analyses between these mean difference potentials and behavioral performance values. The correlation between the measures across different 6 conditions (2 polarities × 3 SOAs) was evaluated via linear regression fits having intercept and slope as coefficients.

## Results

### Behavioral pre-study

Figure 2 shows the difference ( $\Delta$ ) performance values for each polarity condition as a function of SOA. For the same polarity condition, we obtained a typical U-shaped (type B)

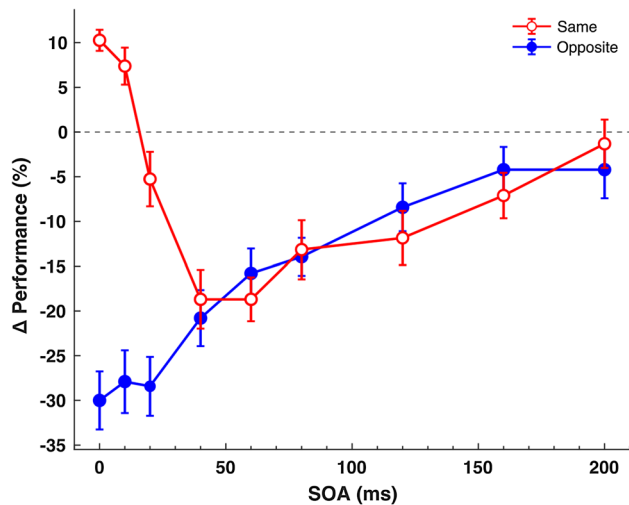


**Fig. 2** Masking magnitude as a function of SOA for same and opposite polarities ( $n = 19$ ). Masking magnitude is given in terms of  $\Delta$  performance values, the change of performance on a masked target relative to that obtained with an unmasked target-only condition (dashed line). Error bars correspond to standard error ( $\pm$  SEM) across observers

function, with performance values (i.e., target visibilities) dropping to a minimum at intermediate SOAs around 50 ms. For short SOAs (0 and 10 ms) of this polarity condition, one observes even an enhancement rather than a suppression of performance. A change in mask polarity led to major changes in the masking function. We found a substantial amount of metacontrast for the opposite polarity condition, but the performance values as a function of SOA pointed out a monotonically increasing (type A) function. The target visibility was minimum at short SOA values (0–20 ms range) and increased monotonically as the SOA between target and mask increased. To assess these modulations in performance values and hence target visibilities, we performed a two-way repeated-measures ANOVA with SOA and polarity (same vs. opposite) as factors. The main effects of SOA ( $F_{8,144} = 10.76$ ,  $p < 0.001$ ,  $\eta_p^2 = 0.374$ ), and polarity ( $F_{1,18} = 86.52$ ,  $p < 0.001$ ,  $\eta_p^2 = 0.828$ ) were significant. Moreover, the two-way interaction between SOA and polarity was also significant ( $F_{8,144} = 27.25$ ,  $p < 0.001$ ,  $\eta_p^2 = 0.602$ ), confirming the differential effects of polarity on the morphology of masking function.

What is notable in comparing the same vs. opposite contrast polarity conditions is that the two masking functions are essentially similar for SOA values around 50 ms and higher, whereas the opposite mask polarity shifts the performance downward for shorter SOA values generating a type A as opposed to type B masking function. Similar effects were observed when mask energy increased (Breitmeyer and Ogmen 2006) and we will revisit this observation when we interpret our results. To examine these modulations of metacontrast in the spatiotemporal profile of the cortical activity, we determined three critical SOA values to be employed in the EEG recordings. When the SOA value was around 10 ms, the target was visible and greatly suppressed in the same and opposite polarity conditions, respectively. This suggests a major change in the amount of masking due to polarity at 10 ms SOA. On the other hand, for SOA values around 50 ms, there was inhibition in both conditions and the amount of inhibition was almost the same. The target became visible (i.e., no masking) at 200 ms SOA value in both polarity conditions. Therefore, these SOA values (10, 50, 200 ms) were used in the main EEG experiment.

## EEG study

### Behavioral results

The trials excluded during the EEG preprocessing stage were not used for the analysis of behavioral data here (Fig. 3). As in pre-study, the ANOVA test revealed significant main effects of SOA ( $F_{2,26} = 38.17$ ,  $p < 0.001$ ,  $\eta_p^2 = 0.746$ ) and polarity ( $F_{1,13} = 111.9$ ,  $p < 0.001$ ,  $\eta_p^2 = 0.896$ ). More importantly, the interaction between these factors

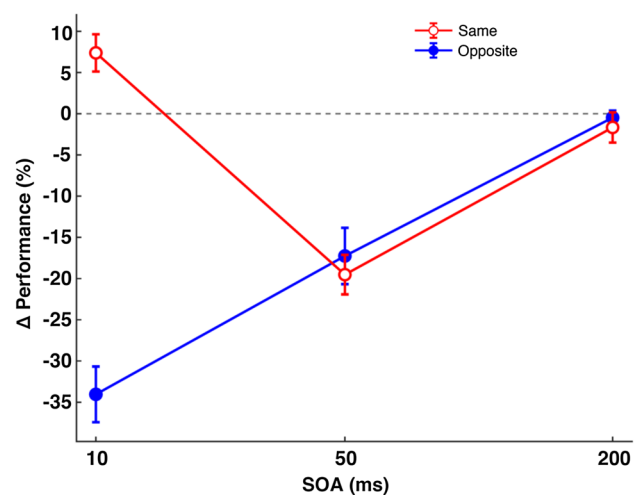


**Fig. 3** Behavioral results of the main EEG experiment ( $n=14$ ).  $\Delta$  performance values for different polarity and SOA conditions. The target-only (T) condition corresponds to the baseline zero level (dashed line). Error bars correspond to standard error ( $\pm$  SEM) across observers

was also significant ( $F_{2,26} = 77.78$ ,  $p < 0.001$ ,  $\eta_p^2 = 0.857$ ). Follow-up pairwise comparisons showed that the target visibility between the two polarity conditions was significantly different only at 10 ms SOA (Bonferroni corrected  $p < 0.001$ ). These behavioral results confirm that the main characteristics of metacontrast masking functions were preserved during the EEG recordings.

### ERP results

For each SOA condition, we performed cluster-based permutation tests to compare difference waveforms [TM – (T + M – NS)] across polarity conditions. These tests revealed only spatiotemporal clusters associated with the significant main effect of polarity (same vs. opposite) when the SOA was 10 ms. In the early ERP component range (160–300 ms), differences between the two polarity conditions (cluster-level  $t_{\text{sum}} = -1224$ ,  $p = 0.014$ ) were mainly clustered over occipital and parieto-occipital scalp sites (Fig. 4a). Within this time-range, the averaged difference potentials for the same polarity condition were more negative compared to those of opposite polarity. The cluster-permutation test revealed additional modulations within the range of late potentials (300–550 ms, cluster-level  $t_{\text{sum}} = 8149$ ,  $p = 0.0002$ ). The same and opposite polarity conditions led to positive and negative mean (difference) potentials, respectively. The spatiotemporal cluster associated with the significant polarity effect was mainly over parietal sites and spread over central and parieto-occipital electrodes (Fig. 4b). Moreover, we applied a cluster-based permutation test to the evoked

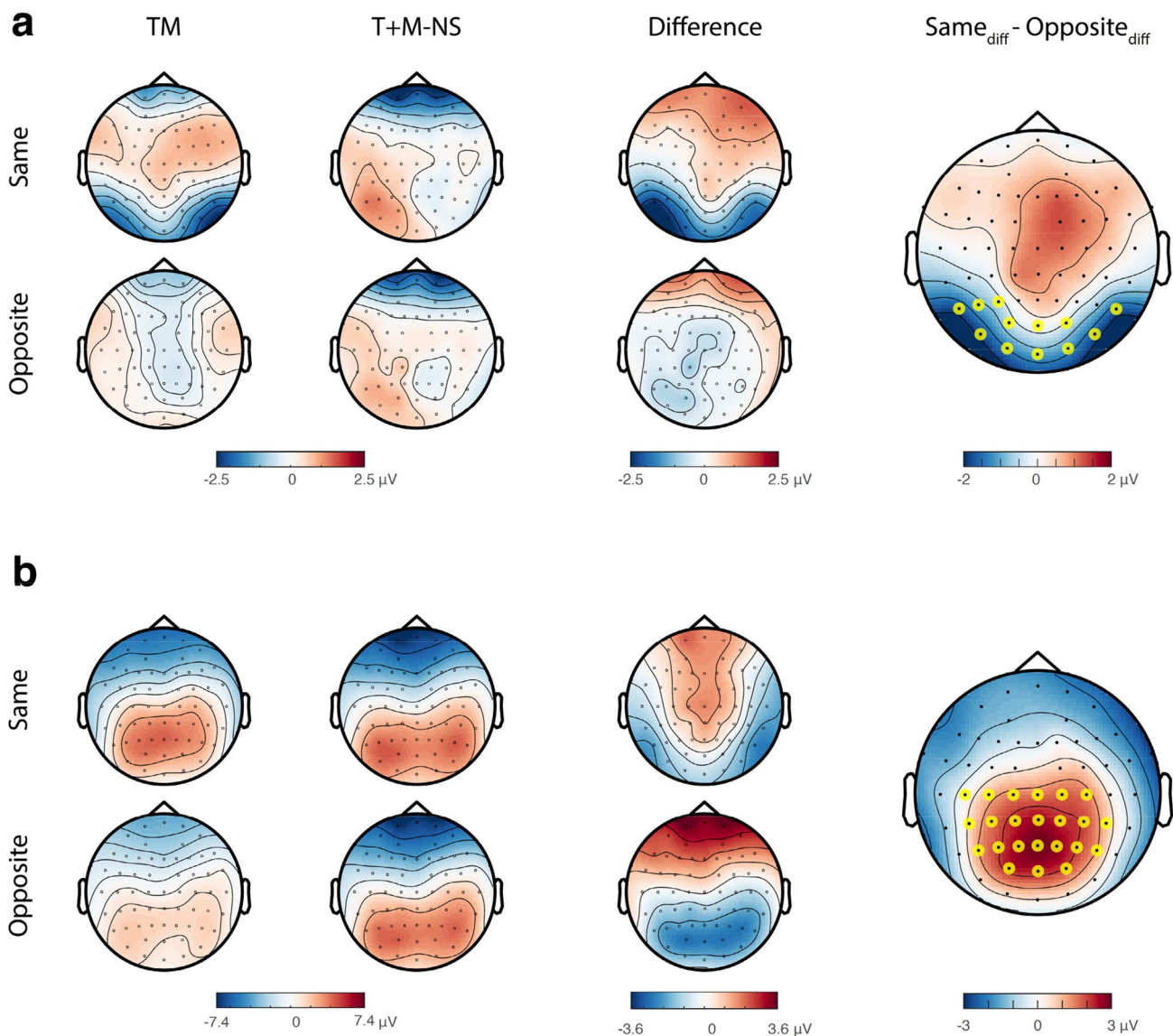


**Fig. 4** Voltage topographical maps of the grand averaged waveforms within the identified time windows for 10 ms of SOA. **a** Early cluster time-range (160–300 ms). **b** Late cluster time-range (300–550 ms). The voltage topographical map of each polarity condition is shown in separate rows. The averaged activities of TM, corresponding synthetic (T+M – NS) waveform, and the difference between them are displayed on the maps in separate columns. The result of the cluster-

based permutation test comparing the difference waveform of two polarity conditions (same<sub>diff</sub> vs. opposite<sub>diff</sub>) is indicated in the last column. The electrodes (i.e., exemplar sites), which were part of the significant spatiotemporal cluster when it was at its largest spatial extent (in terms of the number of electrodes), are marked by yellow-filled circles on the last topographical map

activities to the mask-only (white/same: M+, black/opposite: M–) conditions. A comparison of evoked activities to white mask with those to the black mask did not reveal any significant cluster associated with the polarity effect. Lack of any significant modulations at the cluster-level statistics indicated that the observed effects of polarity on the difference waveforms are not driven by just changes in mask-only conditions and highlight the importance of neural activities driven by both target and mask stimulation (i.e., TM) and their interactions.

As exemplar sites, we identified the electrodes of a significant cluster when it was at its largest spatial extent. We used these electrodes to illustrate the nature of polarity effects on the ERPs. In the early cluster time-range (160–300 ms), there was a robust evoked activity in TM conditions of all SOA conditions (Fig. 5a). This negative component peaked around 200 ms. A similar activity profile was present in the target-only and mask-only conditions (Fig. 5c). However, the duration of negative component was shorter for the target-only condition. Moreover, the amplitudes of all components

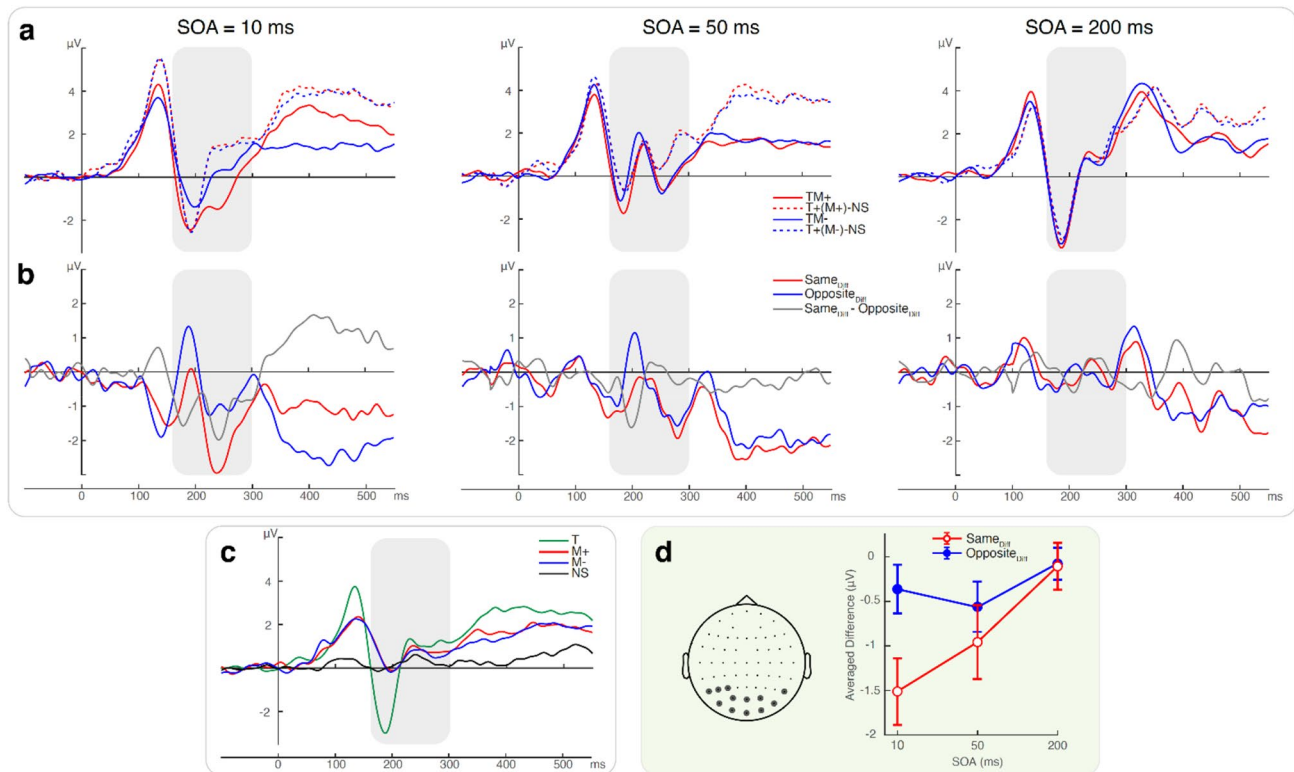


**Fig. 5** Averaged activities and derived waveforms from the exemplar scalp sites ( $n=14$ ). The exemplar sites for the early cluster (160–300 ms) consisted of all the electrodes highlighted in Fig. 4a. The activities for each SOA condition are shown in separate columns. In each plot, the activities of the same and opposite polarity conditions are displayed with red and blue curves, respectively. The 0 ms on the time axis represent the target-onset and corresponding event marker in target-absent trials (i.e., M+, M– and NS). The identified time window based on the cluster-based permutation test is highlighted by a gray rectangle. **a** The grand-averaged ERPs for TM and the corre-

were smaller for the mask-only conditions. Figure 5b indicates the derived difference waveforms [i.e.,  $TM - (T + M - NS)$  reflecting the nonlinear interaction between the target and mask] for all polarity and SOA conditions. At 10 ms SOA condition, the difference between the two polarity conditions ( $same_{diff}$  vs.  $opposite_{diff}$ ) was large, and the same polarity condition ( $same_{diff}$ ) had more negative potentials. As the SOA was increased, the difference between the two polarity conditions became smaller. We averaged these derived waveforms within the identified time-range to further understand the polarity and SOA dependency (Fig. 5d). Compared to the difference performance values, the sign of the difference between the two polarities was in the opposite direction at 10 ms SOA value such that the same polarity led to larger difference potentials (Figs. 3 vs. 5d). Similarly, the morphology of masking functions (i.e., SOA dependency) based on these derived waveforms was different for each polarity condition. In contrast to behavioral performance values, the same and opposite polarity

sponding synthetic ERPs ( $T + M - NS$ ) are time-locked to the onset of the target. **b** The difference waveforms [ $TM - (T + M - NS)$ ] for each polarity condition. The final differences between the two polarity conditions ( $same_{diff} - opposite_{diff}$ ) are also shown by gray curves. **c** The grand-averaged ERPs for target-only (T), mask-only (M+, M–), and no stimulus (NS) conditions. **d** The averaged difference [ $TM - (T + M - NS)$ ] waveforms within the identified time-range are displayed as a function of SOA. The open (red) and filled (blue) circles correspond to the same and opposite polarity conditions, respectively. Error bars represent standard error ( $\pm$  SEM) across observers

conditions led to type A and type B (U-shaped) functions, respectively.

Using the same approach and exemplar sites in Fig. 4b, we computed the averaged activities for different conditions (Fig. 6). In the late cluster time-range (300–550 ms), a positive component (late potentials, LP) were dominant in almost all stimulation configurations (Fig. 6a, c). For SOA of 10 ms, the positive components elicited by target-mask (TM) stimulation were higher and lower than the corresponding synthetic ERPs ( $T + M - NS$ ) of the same and opposite polarity conditions, respectively. This led to positive and negative difference waveforms in this time-range for the same and opposite polarities (Fig. 6b). As the SOA was increased, the positive activities of both target-mask (TM+, TM–) stimulation were lower than the corresponding synthetic ERPs, and hence (almost identical) negative difference waveforms were observed for both polarity conditions ( $same_{diff}$  vs.  $opposite_{diff}$ ). The mean difference potentials in the 300–550 ms range are

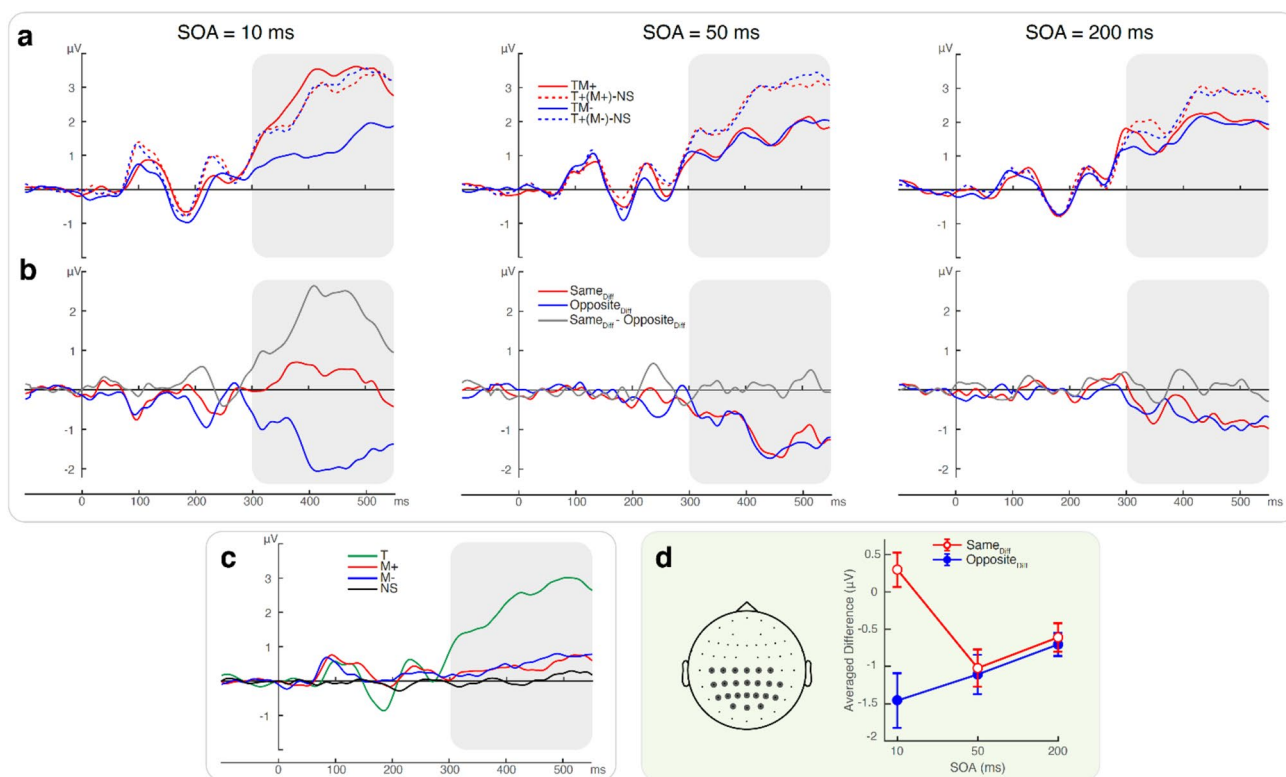


**Fig. 6** Averaged activities and derived waveforms from the exemplar scalp sites ( $n=14$ ). The exemplar sites for the later cluster (300–550 ms) consisted of all the electrodes highlighted in Fig. 4b. The

identified time window is highlighted by a gray rectangle. Other conventions are the same as those in Fig. 5

also displayed as a function of SOA in Fig. 6d. Compared to the early cluster range, the difference between the polarity conditions of 10 ms SOA became larger. Moreover, the morphologies of masking functions (i.e., SOA dependency) were similar to those revealed by behavioral performance values (Figs. 3 vs. 6d). The same and opposite polarity conditions led to type B (U-shaped) and type A functions, respectively.

To better understand and evaluate the relationship between difference potentials and performance values, we additionally performed linear regression fits for both early (Fig. 5d) and late cluster (Fig. 6d) time-range. For the early cluster, the analyses did not reveal a significant correlation between these measures ( $R^2_{\text{adj}} = -0.190$ ,  $p = 0.677$ ; Fig. 7, left plot). On the other hand, there was a robust correlation between the difference potentials of the late cluster and the difference ( $\Delta$ ) performance values ( $R^2_{\text{adj}} = 0.773$ ,  $p = 0.013$ ; Fig. 7, right plot). As the mean potential values increased, the delta performance values increased from negative to positive values. The outcome of these analyses suggests a strong relationship between the modulations of the late positivity and the magnitude and direction of the masking effect.

## Discussion

Using a metacontrast paradigm combined with EEG recording, we investigated the neural correlates of visual masking across different contrast polarities. We employed a contour discrimination task under the same and opposite target-mask polarity conditions. Behavioral results indicated significant differences between the two polarity conditions for SOA values shorter than 50 ms. In this SOA range, the target visibility was strongly suppressed in the opposite polarity condition compared to the target-only and same polarity conditions. Our ERP analyses revealed an early (160–300 ms) and a late (300–550 ms) spatiotemporal cluster associated with the significant effect of polarity. The early cluster was mainly over occipital and parieto-occipital scalp sites. On the other hand, the late modulations of the evoked activities were centered over parietal and centro-parietal sites. With the perspective and framework provided by previous research on masking, we discuss the specific implications of these findings in the following sub-sections.

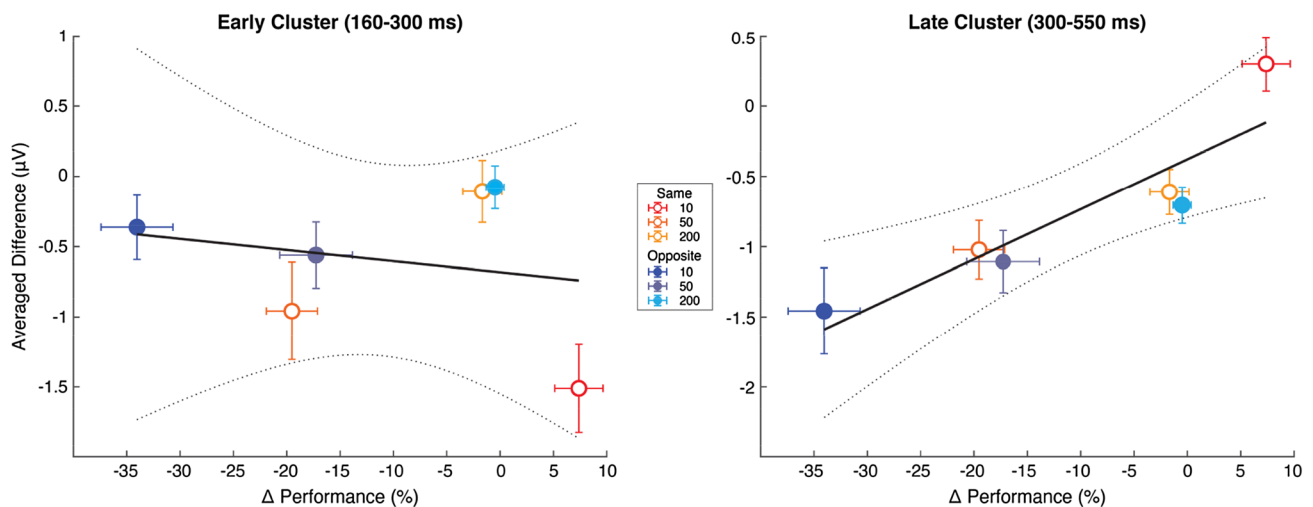


**Fig. 7** Averaged difference activities in the early (left plot) and late cluster (right plot) time-range with the  $\Delta$  performance values for each condition (2 polarities  $\times$  3 SOAs). In each plot, the open and filled symbols display the same and opposite polarity conditions, respec-

tively. Vertical and horizontal error bars correspond to the variance across observers ( $\pm$  SEM). The black solid line indicates the best linear fit and dotted lines denote the 95% confidence intervals on the linear fit

### Metacontrast masking across different polarities

In agreement with previous research (Breitmeyer 1978a; Breitmeyer et al. 2008), we found significant effects of polarity on metacontrast masking. Although previous behavioral studies revealed an overall decrease in the amount of masking when the target and mask had the opposite contrast polarity, they reported U-shaped (type B) masking functions in all the conditions. The contrast polarity did not alter the overall morphology of the masking function in these studies. On the other hand, our findings here indicate that a change in mask polarity can also lead to major changes in the general morphology of the masking function. We found a typical type B metacontrast function in the same polarity condition, whereas a monotonic type A function was present for the opposite polarity. It is unlikely that these changes are due to the differences in criterion contents since we adapted the contour discrimination task of Breitmeyer (1978a). In a first-order luminance-defined stimulation like here, a transition from type B to type A masking function is mostly observed when the mask-to-target (M/T) energy ratio is increased (Breitmeyer 1978b; Growney and Weisstein 1972; Stewart and Purcell 1974). For small M/T ratio values (i.e.,  $< 1$ ), type B (U-shaped) metacontrast functions are typically obtained. As the mask duration or contrast is increased to have a bigger M/T ratio, the strength of masking increases at short SOA values. This transition finally results in strong metacontrast at 0 ms SOA and a monotonically increasing type A function. Furthermore, as mask energy is increased, the transition from type B to type A masking function follows a very similar pattern to the transition we have observed here. For example, Breitmeyer (1978b) kept the target duration at

16 ms and studied metacontrast functions by manipulating mask energy via mask durations ranging from 1 to 32 ms. Increasing the duration/energy of the mask produced gradually stronger masking effects as expected. For mask energies close to target energies (mask durations of 8, 16, and 32 ms), typical type B masking functions with maximum suppression around 60 ms SOA were observed. Increasing the mask energy caused the masking function to change from type B to type A. More importantly, this change occurred in such a way that masking functions remained identical for SOAs longer than 60 ms, but increased masking occurring for SOAs shorter than 60 ms. Similar modulations were obtained through additional comprehensive experiments (Breitmeyer and Ogmen 2006; see Fig. 2.7).

The dual-channel approach successfully explains the shift from a type B to a monotonic type A function. Compared to P cells, the response of M cells saturates at lower stimulation levels (Kaplan and Shapley 1986). Therefore, increasing mask energy (i.e., M/T energy ratio) to higher values mainly favors sustained parvocellular activity and the intra-channel inhibition, which is dependent on this activity. The intra-channel inhibition becomes relatively dominant at short SOA values when the M/T energy ratio becomes higher. That is to say, the monotonic type A function is associated with the stronger sustained signals elicited by the mask and the interference of this activity with that of the target. Based on this explanation, one can hypothesize that the type A function in the opposite polarity condition is mainly due to an increase in the intra-channel inhibition at short SOA values. Since we used the same M/T energy ratio for the same and opposite polarity conditions, such an increase in inhibition may be due to distinct characteristics of cross-polarity (ON vs.

OFF) interaction between the sustained activities. Compared to sustained inhibition within the ON pathway of the same polarity condition, the opposite polarity condition may elicit sustained inhibition across ON and OFF pathways, which has distinct temporal dynamics and strength. Previous studies on other aspects of vision also highlight the dominance of OFF activity in the primary visual cortex and distinct temporal dynamics of across pathway mechanisms (e.g., Jansen et al. 2019; Komban et al. 2014; Oluk et al. 2016). Besides changes in the morphology of masking functions, different mask polarities led to suppression and enhancement in target visibility at short SOAs (i.e., SOAs  $\leq 20$  ms). Interestingly, the same mask polarity increased the target visibility in this SOA range. An important question to ask is whether the facilitatory mechanisms proposed to take place in short and/or negative (i.e., paracontrast) SOAs have a role in this enhancement (Bachmann 1988, 1994; Kafaligönül et al. 2009; Wutz et al. 2018). Future research, including systematic manipulations of polarity, M/T energy ratio (e.g., changes in duration or contrast), and criterion content, will be informative to have a better understanding of across and within pathway interactions in the temporal domain.

### Event-related potentials: masking

Our results revealed ERP modulations beyond 160 ms under different metacontrast conditions. The earliest modulation over the visual cortex (occipital and parieto-occipital scalp sites) was within the 160–300 ms time-range. Therefore, these ERP findings highlight the recurrent/reentrant nature of metacontrast rather than the fast feedforward sweep (Bridgeman 1988; Haynes et al. 2005; Kafaligonul et al. 2015; Lamme and Roelfsema 2000; Railo and Koivisto 2009). According to the aforementioned studies above, a shift from type B to type A masking function in behavioral performance has been interpreted as an increase in sustained inhibition at short SOA values. Given also that we identified the clusters and ERP modulations through comparing polarity conditions at SOA of 10 ms, these ERP modulations can be specifically interpreted as an indication of changes in recurrent inhibition (rather than changes in early lateral inhibition) within the sustained P channel (Breitmeyer et al. 2006; Ogmen et al. 2003). It should be also noted that the modulations of both early and late clusters were not restricted to 10 ms SOA value. Notably, the modulations in the late positivity (300–550 ms) reflected the overall morphology of masking functions. The changes in the mean difference waveforms as a function of SOA were in line with the masking functions based on performance values. It has been proposed that inter-channel inhibition between M and P pathways become dominant around 50 ms SOA (Breitmeyer and Ogmen 2000). Although there was no difference between the two polarity conditions, the averaged values of

both clusters deviated from baseline zero level, suggesting a significant nonlinear interaction at this SOA.

Backward masking and metacontrast paradigms have been commonly employed in visual awareness studies since systematic manipulations in SOA lead to aware and unaware (i.e., unmasked and masked) conditions (e.g., Railo and Koivisto 2009). The difference between the evoked activities of these conditions (unmasked – masked) typically peaks around 200–250 ms over occipital and posterior temporal sites. This difference waveform correlates with the appearance of a stimulus in visual awareness, and it has been named visual awareness negativity (VAN, see Koivisto and Revonsuo 2010 for a review). VAN has also been associated with recurrent processing between occipital and temporal sites. This negativity is typically followed by a later positivity (LP) beyond 300 ms in the difference waveforms over parietal sites. LP has been suggested to reflect the conscious processing of the seen stimulus. In terms of spatiotemporal profile on the neural activity (e.g., time-range, scalp sites), the early negative and late positive clusters in the current study are strikingly similar to VAN and LP, respectively (see also Koivisto and Revonsuo 2010; for typical VAN and LP characteristics). Similarly, our ERP findings are also in line with those described by Del Cul et al. (2007). In their backward masking paradigm, a target number was masked with four surrounding and non-overlapping letters. Compared to the target duration (16 ms), the mask duration was much higher (200 ms) to have a high M/T energy ratio. As expected from previous metacontrast findings, they got a monotonic type A masking function of behavioral performance. Similar to our observations here, the ERP analyses pointed out separate and distinct stages in target-mask interactions by revealing early (140–270 ms) and late ( $> 270$  ms) modulations. In the early time-range, the results indicated a progressive build-up of a nonlinear activation as a function of SOA over posterior occipito-temporal and parietal sites, suggesting a dynamic nonlinear amplification as the neural correlate of masking strength. On the other hand, the late nonlinear modulations were associated with more distributed fronto-parietal-temporal activation. In addition to being sigmoidally dependent on SOA, they were also correlated with the subjective visibility reports (i.e., target seen/not-seen trials). Building from these findings, they suggested that the early interactions represent subliminal recurrent processing over occipital-temporal sites whereas the later ones correspond to the neural correlate of conscious reports.

Through reanalyses of data by Jeffrey and Musselwhite (1986), Bridgeman (1988) demonstrated U-shaped dependency (type B) of averaged EEG activities around 250 ms, suggesting that the components in this range reflecting the perceptual effects of metacontrast. Using a more comprehensive design including both mask and pseudo-mask conditions, Van Aalderen-Smeets et al. (2006) further

investigated metacontrast with MEG. As opposed to the U-shaped dependency in the mask conditions, the behavioral performance values in the pseudomask conditions were nearly perfect and almost constant across different SOA values. The averaged potentials around 250 ms had a U-shaped dependency on SOA for both mask and pseudomask conditions (see also Railo and Koivisto 2009). On the other hand, the activities around 340 ms indicated a clear distinction between mask and pseudomask conditions and mainly overlapped with the behavioral performance values. Our findings here extend these observations by showing that the masking functions derived from the early component significantly deviated from those of behavioral performance values. As opposed to the masking functions derived from performance values, we even observed type A and type B (U-shaped) functions for the same and opposite polarity conditions (Fig. 5d). On the other hand, the averaged activities of the late positivity were significantly correlated with the changes in behavioral performance values and reflected overall metacontrast masking effects. Within the context of metacontrast masking, these results together with previous research highlight the importance of LP in reflecting perceptual changes. Of note, there has been an ongoing debate whether the early VAN or late LP reflects the neural correlates of consciousness and awareness (see Förster et al. 2020 for a recent review). Some of the previous awareness and consciousness studies provide supporting evidence that LP does not reflect conscious perception but just the behavioral report of participants (e.g., Pitts et al. 2014). In these studies, either spatially overlapping masks or other experimental paradigms (e.g., inattention blindness as in Pitts et al. 2014) have been mainly used. To generate aware and unaware conditions, these designs typically included a distinct SOA condition. Therefore, they do not provide a framework to evaluate the morphology of masking functions across different ERP components. Further systematic investigations will be helpful to have a better characterization of the identified ERP components within the context of visual masking.

### Event-related potentials: ON and OFF pathway interactions

Besides invasive neurophysiological recordings in the primary visual cortex, previous research also focused on understanding whether distinct characteristics of ON and OFF pathways can be identified at the population level via EEG (e.g., Zemon et al. 1988; Zemon and Gordon 2006). Separate luminance increment and decrement stimulation have been designed to reveal these characteristics and the contributions of ON and OFF pathways to the human cortical responses. In general, the findings indicate that the luminance decrements elicit higher amplitude VEPs (visual evoked potentials) over

occipital scalp sites, suggesting OFF pathway dominance in the visual cortex. Using sawtooth stimulation with a low temporal frequency, Norcia et al. (2020) have recently provided a detailed timeline of such dominance. Compared to increments, the evoked potentials within the 100–200 ms range (i.e., negative component peaks around 150 ms) were larger in amplitude and shorter in latency for luminance decrements. Prior studies have also combined the sawtooth temporal stimulation profile with an adaptation design. For instance, Roveri et al. (1997) examined adaptation-induced changes in the VEPs to a test stimulus, which is either a luminance increment (ON) or decrement (OFF). Similarly, the adaptation conditions also included two polarity conditions (i.e., 2 adapters  $\times$  2 test conditions). The results revealed selective aftereffects on the 100–200 ms time-range (N1-P1 component range), which provides some supporting evidence for separate processing of increments and decrements. More importantly, the cross polarity adaptation conditions, which are suggested to engage cortical interactions between ON and OFF pathways, indicated distinct changes in the neural activity up to 300 ms. In the present study, a comparison of evoked activities to the white and black masks did not reveal any cluster associated with the effect of contrast polarity. However, when this stimulation was combined with a 10 ms preceding white target, the changes became differential and led to an early and late cluster associated with the effect of polarity. Notably, the time-range of early cluster overlaps the modulations in the cross-polarity adaptations of Roveri et al. (1997). Together with previous research, our findings highlight the importance of early cluster time-range to understand the nature of ON–OFF pathway interactions at the population level in the visual cortex. Based on our interpretation of masking functions and ERP components above, the modulations in this time-range may reflect inhibitory mechanisms across polarities within the P channel (e.g., inhibition between on-sustained and off-sustained populations). Further investigation of this critical time-range via metacontrast may shed light on the nature of cross-polarity interactions in the summed cortical activity.

### Conclusions

In conclusion, our study points to robust effects of contrast polarity on metacontrast in both behavioral performance and ERP components. The behavioral findings provide evidence for the first time that a change in contrast polarity can even shift masking function from a type B (U-shaped) to a type A monotonic increasing function. This finding suggests that stronger responses elicited by the OFF-pathway, compared to the ON-pathway, increase intrachannel sustained inhibition in a way similar to the case when mask energy is increased in the same-polarity metacontrast. Our ERP analyses revealed

two spatiotemporal clusters beyond 160 ms associated with the effect of polarity. In terms of spatiotemporal profiles, these identified clusters with a low-level stimulus manipulation (i.e., contrast polarity) were strikingly similar to those previously described by other masking studies with different designs. Although these behavioral and ERP findings do not rule out other proposed mechanisms for metacontrast (i.e., interchannel inhibition), they highlight that the late recurrent inhibitions within the sustained P channel also play an important role in metacontrast masking.

**Acknowledgements** We would like to thank Utku Kaya for suggestions on the data analyses. We are also grateful to the anonymous reviewers whose detailed and helpful comments significantly improved our manuscript.

**Funding** This work was supported by The Scientific and Technological Research Council of Turkey (TUBITAK, Grant Number 119K368).

**Data availability** The dataset is available from the corresponding author on request. Any access to the data will be granted in accordance with the informed consent signed by the participants.

## Declarations

**Conflicts of interest** The authors have no actual or potential conflicts of interest.

**Ethical approval** All experimental procedures were in accordance with the Declaration of Helsinki and international guidelines and approved by the local ethics committee.

**Informed consent** Informed consent was obtained from all individual participants included in the study.

## References

- Akyuz S, Pavan A, Kaya U, Kafaligonul H (2020) Short- and long-term forms of neural adaptation: an ERP investigation of dynamic motion aftereffects. *Cortex* 125:122–134
- Bachmann T (1988) Time course of the subjective contrast enhancement for a second stimulus in successively paired above-threshold transient forms: perceptual retouch instead of forward masking. *Vis Res* 28:1255–1261
- Bachmann T (1994) *Psychophysiology of visual masking: the fine structure of conscious experience*. Nova Science Publishers, Commack, NY
- Bachmann T, Francis G (2013) *Visual masking: studying perception, attention, and consciousness*. Academic Press, Oxford, UK
- Brainard D (1997) The psychophysics toolbox. *Spat Vis* 10:433–436
- Breitmeyer BG (1978a) Metacontrast with black and white stimuli: evidence of inhibition of on and off sustained activity by either on or off transient activity. *Vis Res* 18:1443–1448
- Breitmeyer BG (1978b) Metacontrast masking as a function of mask energy. *Bull Psychon Soc* 12:50–52
- Breitmeyer BG, Ogmen H (2000) Recent models and findings in visual backward masking: a comparison, review, and update. *Percept Psychophys* 62:1572–1595
- Breitmeyer BG, Ogmen H (2006) *Visual masking: time slices through conscious and unconscious vision*, 2nd edn. Oxford University Press, Oxford, UK
- Breitmeyer BG, Ogmen H, Chen J (2004) Unconscious priming by color and form: different processes and levels. *Conscious Cogn* 13:138–157
- Breitmeyer BG, Kafaligönül H, Ögmen H, Mardon L, Todd S, Ziegler R (2006) Meta- and paracontrast reveal differences between contour and brightness processing mechanisms. *Vis Res* 46:2645–2658
- Breitmeyer BG, Tapia E, Kafaligönül H, Ögmen H (2008) Metacontrast masking and stimulus contrast polarity. *Vis Res* 48:2433–2438
- Bridgeman B (1988) Visual evoked potentials: concomitants of metacontrast in late components. *Percept Psychophys* 43:401–403
- Cecere R, Gross J, Willis A, Thut G (2017) Being first matters: topographical representational similarity analysis of ERP signals reveals separate networks for audiovisual temporal binding depending on the leading sense. *J Neurosci* 37(21):5274–5287
- Del Cul A, Baillet S, Dehaene S (2007) Brain dynamics underlying the nonlinear threshold for access to consciousness. *PLoS Biol* 5:2408–2423
- Donchin E, Wicke JD, Lindsley DB (1963) Cortical evoked potentials and perception of paired flashes. *Science* 141(3587):1285–1286
- Dow BM (1974) Functional classes of cells and their laminar distribution in monkey visual cortex. *J Neurophysiol* 37:927–946
- Fahrenfort JJ, Scholte HS, Lamme VAF (2007) Masking disrupts reentrant processing in human visual cortex. *J Cogn Neurosci* 19:1488–1497
- Förster J, Koivisto M, Revonsuo A (2020) ERP and MEG correlates of visual consciousness: the second decade. *Conscious Cogn* 80:102917
- Francis G (2000) Quantitative theories of metacontrast masking. *Psychol Rev* 107:768–785
- Growney R, Weisstein N (1972) Spatial characteristics of metacontrast. *J Opt Soc Am* 62(5):690–696
- Haynes J-D, Driver J, Rees G (2005) Visibility reflects dynamic changes of effective connectivity between V1 and fusiform cortex. *Neuron* 46:811–821
- Hubel DH, Wiesel TN (1968) Receptive fields and functional architecture of monkey striate cortex. *J Physiol* 195:215–243
- Jansen M, Jin J, Li X, Lashgari R, Kremkow J, Bereshpolova Y, Swadlow HA, Zaidi Q, Alonso JM (2019) Cortical balance between ON and OFF visual responses is modulated by the spatial properties of the visual stimulus. *Cereb Cortex* 29(1):336–355
- Jeffreys DA, Musselwhite MJ (1986) A visual evoked potential study of metacontrast masking. *Vis Res* 26:631–642
- Kafaligönül H, Breitmeyer BG, Ögmen H (2009) Effects of contrast polarity in paracontrast masking. *Atten Percept Psychophys* 71(7):1576–1587
- Kafaligonul H, Breitmeyer BG, Ögmen H (2015) Feedforward and feedback processes in vision. *Front Psychol* 6:279
- Kaplan E, Shapley RM (1986) The primate retina contains two types of ganglion cells, with high and low contrast sensitivity. *Proc Natl Acad Sci USA* 83(8):2755–2757
- Kaya U, Kafaligonul H (2019) Cortical processes underlying the effects of static sound timing on perceived visual speed. *Neuroimage* 199:194–205
- Kleiner M, Brainard D, Pelli D (2007) What's new in Psychtoolbox-3? *Perception* 36(14):1–16
- Koivisto M, Grassini S (2016) Neural processing around 200 ms after stimulus-onset correlates with subjective visual awareness. *Neuropsychologia* 84:235–243
- Koivisto M, Revonsuo A (2010) Event-related brain potential correlates of visual awareness. *Neurosci Biobehav Rev* 34:922–934
- Komban SJ, Kremkow J, Jin J, Wang Y, Lashgari R, Li X, Zaidi Q, Alonso JM (2014) Neuronal and perceptual differences in the temporal processing of darks and lights. *Neuron* 82:224–234

- Lamme VAF, Roelfsema PR (2000) The distinct modes of vision offered by feedforward and recurrent processing. *Trends Neurosci* 23:571–579
- Maris E, Oostenveld R (2007) Nonparametric statistical testing of EEG- and MEG-data. *J Neurosci Methods* 164(1):177–190
- Norcia AM, Yakovleva A, Hung B, Goldberg JL (2020) Dynamics of contrast decrement and increment responses in human visual cortex. *Transl Vis Sci Technol* 9(10):6
- Ogmen H, Breitmeyer BG, Melvin R (2003) The what and where in visual masking. *Vis Res* 43:1337–1350
- Oluk C, Pavan A, Kafaligonul H (2016) Rapid motion adaptation reveals the temporal dynamics of spatiotemporal correlation between ON and OFF pathways. *Sci Rep* 6:34073
- Pelli D (1997) The VideoToolbox software for visual psychophysics: transforming numbers into movies. *Spat Vis* 10:437–442
- Pitts MA, Padwal J, Fennelly D, Martínez A, Hillyard SA (2014) Gamma band activity and the P3 reflect post-perceptual processes, not visual awareness. *Neuroimage* 101:337–350
- Railo H, Koivisto M (2009) The electrophysiological correlates of stimulus visibility and metacontrast masking. *Conscious Cogn* 18:794–803
- Rieger JW, Braun C, Bühlhoff HH, Gegenfurtner KR (2005) The dynamics of visual pattern masking in natural scene processing: a magnetoencephalography study. *J Vis* 5(3):275–286
- Roveri L, Demarco PJ, Celesia GG (1997) An electrophysiological metric of activity within the ON- and OFF-pathways in humans. *Vis Res* 37:669–674
- Schiller PH (1982) Central connections to the ON- and OFF-pathways. *Nature* 297:1288–1374
- Schiller PH (1992) The ON and OFF channels of the visual system. *Trends Neurosci* 15:86–92
- Schiller P, Chorover L (1966) Metacontrast: its relation to evoked potentials. *Science* 153:1398–1400
- Schiller PH, Finlay BL, Volman SF (1976) Quantitative studies of single cell properties in monkey striate cortex. I–V. *J Neurophysiol* 39:1288–1374
- Sherrick MF, Keating JK, Dember WN (1974) Metacontrast with black and white stimuli. *Can J Psychol* 28:438–445
- Sterkin A, Yehezkel O, Bonneh YS, Norcia A, Polat U (2009) Backward masking suppresses collinear facilitation in the visual cortex. *Vis Res* 49:1784–1794
- Stewart AL, Purcell DG (1974) Visual backward masking by a flash of light: a study of u-shaped detection functions. *J Exp Psychol* 103(3):553–566
- Tadel F, Baillet S, Mosher JC, Pantazis D, Leahy RM (2011) Brainstorm: a user-friendly application for MEG/EEG analysis. *Comput Intell Neurosci* 2011:e879716
- Thaler L, Schütz AC, Goodale MA, Gegenfurtner KR (2013) What is the best fixation target? The effect of target shape on stability of fixational eye movements. *Vis Res* 76:31–42
- Uusitalo MA, Ilmoniemi RJ (1997) Signal-space projection method for separating MEG or EEG into components. *Med Biol Eng Comput* 35(2):135–140
- Van Aalderen-Smeets SI, Oostenveld R, Schwarzbach J (2006) Investigating neurophysiological correlates of metacontrast masking with magnetoencephalography. *Adv Cogn Psychol* 2:21–35
- Walter WG, Cooper R, Aldridge VJ, McCallum WC, Winter AL (1964) Contingent negative variation: an electric sign of sensorimotor association and expectancy in the human brain. *Nature* 203(4943):380–384
- World Medical Association (2013) Declaration of Helsinki: ethical principles for medical research involving human subjects. *JAMA* 310(20):2191–2194
- Wutz A, Melcher D, Samaha J (2018) Frequency modulation of neural oscillations according to visual task demands. *Proc Natl Acad Sci USA* 115:1346–1351
- Zemon V, Gordon J (2006) Luminance-contrast mechanisms in humans: visual evoked potentials and a nonlinear model. *Vis Res* 46:4163–4180
- Zemon V, Gordon J, Welch J (1988) Asymmetries in ON and OFF visual pathways of humans revealed using contrast-evoked cortical potentials. *Vis Neurosci* 1:145–150

**Publisher's Note** Springer Nature remains neutral with regard to jurisdictional claims in published maps and institutional affiliations.